CONFIDENTIAL

Copy 295
RM L55A07

NACA RM L55A07

NACA

RESEARCH MEMORANDUM

EXPERIMENTAL DETERMINATION OF THE AERODYNAMIC DERIVATIVES ARISING FROM ACCELERATION IN SIDESLIP FOR A TRIANGULAR, A SWEPT, AND AN UNSWEPT WING

By Donald R. Riley, John D. Bird, and Lewis R. Fisher

Langley Aeronautical Laboratory
Langley Field, Va.

CLASSIFIED DOCUMENT

This material contains information affecting the National Defense of the United States within the meaning of the espionage laws, Title 18, U.S.C., Secs. 793 and 794, the transmission or revelation of which in any manner to an unauthorized person is prohibited by law.

NATIONAL ADVISORY COMMITTEE FOR AERONAUTICS

WASHINGTON

March 30, 1955

CONFIDENTIAL

NATIONAL ADVISORY COMMITTEE FOR AERONAUTICS

RESEARCH MEMORANDUM

EXPERIMENTAL DETERMINATION OF THE AERODYNAMIC DERIVATIVES ARISING FROM ACCELERATION IN SIDESLIP FOR A TRIANGULAR, A SWEPT, AND AN UNSWEPT WING

By Donald R. Riley, John D. Bird, and Lewis R. Fisher

SUMMARY

A low-speed wind-tunnel investigation has been conducted to determine the aerodynamic derivatives arising from acceleration in sideslip for a 60° triangular, a 45° sweptback, and an unswept wing. Data were obtained through an angle-of-attack range for each of the three wings by forcing each wing to perform a lateral plunging oscillation across the jet of the 6- by 6-foot test section of the Langley stability tunnel.

The magnitude of the sideslip acceleration derivatives encountered and the effect of wing plan form on these derivatives was small in the low angle-of-attack range. In the high angle-of-attack range, the swept and triangular plan forms had values of the sideslip acceleration derivatives that were large in comparison with the other stability derivatives with which they are generally combined in the lateral-stability calculations. These acceleration derivatives increased with angle of attack at a much greater rate for the high angle-of-attack range than for the low angle-of-attack range. The acceleration derivatives for the unswept plan form were small throughout the angle-of-attack range in comparison with the values for the wings with swept and triangular plan forms.

An indication of the effect of changes in frequency on the sideslip acceleration derivatives was obtained for the 60° triangular wing and the results showed that, at high angles of attack, changes in frequency can make rather large differences in the values of the acceleration derivatives. The general trend at these high angles is that the lower frequency corresponded to the larger magnitude of the acceleration derivative.

A comparison of the lateral-stability derivatives C_{n_β} and C_{l_β} obtained from the oscillation tests with static sideslip results indicated agreement at the low angles of attack where the acceleration derivatives were small and a definite departure at the high angles of attack for the

wing of triangular plan form. Similar trends were noted for the swept wing. Agreement was obtained for the unswept wing throughout the angle-of-attack range, indicating that the unsteady effects were small for this wing.

INTRODUCTION

In the most usual type of wind-tunnel oscillation-in-yaw tests, the model is rotated in yaw about its vertical wind axis in the airstream. This motion is a combination of pure yawing and pure sideslipping; hence, the resulting measured damping-in-yaw derivative is the algebraic sum of the coefficients of yawing moment due to yawing velocity C_{n_r} and of yawing moment due to acceleration in sideslip $C_{n_{\dot{\beta}}}$, in the manner $C_{n_r} - C_{n_{\dot{\beta}}}$.

The C_{n_r} due to steady yawing can be measured conveniently by means of the curved-flow test procedure employed in the Langley stability tunnel. The differences between the results of comparative oscillation and curved-flow tests for the same model under the same test conditions yield some information about the magnitude of $C_{n_{\dot{\beta}}}$ relative to C_{n_r}. Several such comparative tests (see refs. 1, 2, and 3, for example) have indicated that, under certain circumstances, $C_{n_r} - C_{n_{\dot{\beta}}}$ can be much different from C_{n_r}. This difference must be attributable in considerable degree to the $C_{n_{\dot{\beta}}}$ derivative, as pointed out in references 1 and 2. Likewise the rolling-moment derivatives C_{l_r} and $C_{l_{\dot{\beta}}}$, that is, the coefficients of rolling moment due to yawing velocity and rolling moment due to acceleration in sideslip, combine in a similar manner for the oscillation-in-yaw tests. Thus, the difference between the combination derivative $C_{l_r} - C_{l_{\dot{\beta}}}$ and the curved-flow derivative C_{l_r} must be attributable in considerable degree to the acceleration derivative $C_{l_{\dot{\beta}}}$.

In addition to wind-tunnel tests, some dynamic-lateral-stability calculations have been performed for several representative airplane models. (For example, see ref. 4.) The results of these calculations indicated that, when the acceleration derivatives were large, large differences in stability occurred depending on whether the acceleration derivatives were included or omitted in the computations. In particular, calculations performed for a model having a 60° triangular wing at a high angle of attack indicated a reversal in dynamic lateral stability from unstable to stable when the estimated acceleration derivatives were included.

In view of the apparent magnitude and importance of the acceleration derivatives, the present investigation was undertaken to evaluate independently the sideslip acceleration derivatives through an angle-of-attack range for three wings of widely different plan form. Data were obtained by forcing these wings to perform, in effect, a lateral plunging oscillation across the jet of the 6- by 6-foot test section of the Langley stability tunnel. The results serve to illustrate the importance of the sideslip acceleration derivatives, particularly in view of their influence on the dynamic lateral stability of aircraft, by indicating the magnitudes of these derivatives that may be encountered for a triangular, a swept, and an unswept wing.

SYMBOLS

The data presented herein are in the form of standard NACA coefficients of forces and moments which are referred to the stability system of axes with the origin located at the quarter chord of the mean aerodynamic chord. The positive directions of forces, moments, and angles are shown in figure 1. The coefficients and symbols are defined as follows:

C_L	lift coefficient, L/qS
C_D	drag coefficient, D/qS where $D = -X$ at $\beta = 0^\circ$
C_Y	lateral-force coefficient, Y/qS
C_m	pitching-moment coefficient, $M/qS\bar{c}$
C_n	yawing-moment coefficient, N/qSb
C_l	rolling-moment coefficient, L'/qSb
L	lift
X	longitudinal force
D	drag
Y	lateral force
M	pitching moment
N	yawing moment

L' rolling moment

L'_o/y_o ratio of rolling-moment amplitude to amplitude of model displacement at any specified time

y lateral displacement of model from tunnel center line

q dynamic pressure, $\frac{1}{2}\rho V^2$

ρ mass density of air

V free-stream velocity

S wing area

$\bar{c}$ mean aerodynamic chord

b span

A aspect ratio

α angle of attack, deg

β angle of sideslip, deg

$\dot{\beta}$ rate of change of angle of sideslip with time, $d\beta/dt$

r angular velocity in yaw

ϕ phase angle between a moment and model displacement, (positive when moment leads displacement)

f frequency of oscillation, cps

$C_{Y_\beta} = \frac{\partial C_Y}{\partial \beta}$ per degree

$C_{n_\beta} = \frac{\partial C_n}{\partial \beta}$ per degree

$C_{l_\beta} = \frac{\partial C_l}{\partial \beta}$ per degree

$C_{n_{\dot{\beta}}} = \frac{\partial C_n}{\partial \frac{\dot{\beta} b}{2V}}$ per radian

$$C_{l_{\dot{\beta}}} = \frac{\partial C_l}{\partial \frac{\dot{\beta} b}{2V}} \text{ per radian}$$

$$C_{n_r} = \frac{\partial C_n}{\partial \frac{rb}{2V}} \text{ per radian}$$

APPARATUS AND MODELS

Apparatus

The oscillation test apparatus constructed for this investigation was, in essence, a simple parallelogram linkage as shown in the photographs of figure 2. This mechanism made use of a 9-foot length of heavy-wall streamlined steel tubing of approximately a 4-inch chord that spanned the jet and extended through the walls of the 6- by 6-foot test section of the Langley stability tunnel. The streamlined strut was supported at either end by swinging arms, triangular in shape and fashioned from circular steel tubing. These triangular arms were pinned at two of their apexes to a rigid tunnel structural member with the third apex pinned to the streamlined strut. The arms and hence the strut were forced to oscillate by the action of a group of springs. Data for the models were obtained by means of a strain-gage balance which was mounted at the top of a 6-inch length of circular steel tubing that was welded to the streamlined strut and braced laterally. The purpose of this vertical support for the strain-gage balance was to elevate the wings above the streamlined strut.

Although it is apparent that a pure lateral oscillatory motion cannot be obtained by such apparatus, the streamwise motion of the model can be minimized to an extent that it can be considered negligible. This was accomplished for these tests by restricting the lateral motion of the model to a maximum amplitude of about 9 inches and by using a radius of the swinging arm of 45 inches.

The rolling and yawing moments, which were measured in this investigation by means of the strain-gage balance during oscillation, provided values of the sideslip oscillatory derivatives C_{n_β}, C_{l_β}, $C_{n_{\dot{\beta}}}$, and $C_{l_{\dot{\beta}}}$. Model displacement was obtained by means of a resistance slide-wire mechanism operated by one of the swinging arms. The strain-gage and slide-wire signals were passed through a set of low-pass filters, which had a cutoff frequency of 10 cycles per second, and then were fed into an amplifier. The amplified signal was used to operate a multichannel ink recorder

that provided the data in the form of oscillatory traces plotted against time. In order to prevent the aerodynamic phase lags from being masked by those introduced by the instrumentation, the filters for the strain-gage and slide-wire circuits were designed to have the same phase lag. Several check tests indicated the phase difference of the various circuits was negligible.

Models

The models used in the present investigation consisted of a 60° triangular, a 45° sweptback, and an unswept wing. The swept and unswept wings had aspect ratios of 4.0, taper ratios of 0.6, and rounded tips. Each of the wings was constructed from 3/4-inch plywood having essentially a flat-plate airfoil section with a circular leading edge and a beveled trailing edge. The trailing edges of all wings were beveled to provide a trailing-edge angle of 10° that was constant across the span. Sketches of the three wings and their geometric characteristics are presented as figure 3. Photographs of the three wings mounted on the oscillation strut are presented in figure 4.

Before testing the models, each wing was statically balanced about the mounting point to eliminate inertia moments from the records. In order to balance the unswept wing in yaw it was necessary to locate an additional small streamlined lead weight on the wing center line approximately 6 inches forward of the leading edge. (See fig. 4(c).) In order to balance all wings about the roll axis when mounted on the strain-gage balance, it was necessary to locate two small lead weights on wooden pylons about three-quarters of an inch below the lower surface of the wing along the Y-axis several inches on either side of the wing center line.

The wings were mounted on a strain-gage balance which, in turn, was fastened rigidly to the oscillation strut. The canopies shown in the photographs of figure 4 were made from balsa wood and served to streamline the protrusion of the strain-gage balance above the upper surface of the wing at angles of attack. All openings in the canopies were sealed to prevent leakage of air through the model.

Tests

Oscillation tests were conducted on each of the three wing models in the 6- by 6-foot test section of the Langley stability tunnel in the following manner. The model was displaced approximately 9 inches from the equilibrium position which corresponded to the tunnel center line, and the tunnel airspeed was then increased to the desired operating dynamic pressure. The model was released by means of a trigger mechanism and

allowed to oscillate. Rolling moment, yawing moment, and model displacement were recorded for the triangular and swept wings in angle-of-attack increments of 4° from $\alpha = 0^\circ$ to $\alpha = 16^\circ$ and thereafter in 2° increments up to $\alpha = 32^\circ$. Data for the unswept wing were obtained in 2° increments from $\alpha = 0^\circ$ to $\alpha = 16^\circ$. The frequency of oscillation of each wing varied somewhat at different angles of attack depending, of course, on the aerodynamic effects encountered. However, for all three wings for the angles of attack investigated, the frequency only varied from approximately 2.15 to 2.45 cycles per second. In order to provide some indication of the effect of changes in frequency of oscillation, additional tests at the same angles of attack were conducted on the 60° triangular wing for a frequency of about 1.4 cycles per second.

Oscillation records were also obtained for every test angle of attack at a tunnel airspeed of zero to ascertain that the wing models were properly balanced to eliminate inertia effects. Several check tests were conducted with a plywood box around the model to insure that still-air aerodynamic-inertial effects did not influence these wind-off tests. (See fig. 5.)

In addition to the oscillation tests, sideslip tests to determine the steady-state values of C_{Y_β}, C_{n_β}, and C_{l_β} through the angle-of-attack range were conducted for each of the three wing models. For these tests the models were mounted on a single vertical support strut and the data were recorded by means of a conventional six-component balance system. The canopies present on all wings for the oscillation tests were also present for these tests; however the small streamlined lead weight on the straight wing located forward of the leading edge and the lead weights mounted on the lower surface of each wing were removed. Data were recorded at sideslip angles of 0° and $\pm 5^\circ$ at the low angles of attack and at 0°, $\pm 2^\circ$, and $\pm 5^\circ$ at the high angles of attack. For the unswept wing, data were obtained in increments of 2° from $\alpha = -4^\circ$ to $\alpha = 16^\circ$ and for the swept and triangular wings from $\alpha = -4^\circ$ to $\alpha = 30^\circ$ and 32°, respectively.

All tests were conducted in the 6- by 6-foot test section of the Langley stability tunnel at a dynamic pressure of 39.7 pounds per square foot which corresponds to a Mach number of 0.17. The Reynolds number based on the mean aerodynamic chord of the wing was approximately 2.1×10^6 for the 60° triangular wing and 0.93×10^6 for the swept and unswept wings.

CORRECTIONS

Jet boundary corrections to angle of attack and drag coefficient, determined by the method of reference 5 and based on the data obtained

from the static sideslip tests at $\beta = 0^{\circ}$, have been applied to both the steady-state and oscillatory results. No corrections were applied to the oscillatory derivatives because they were felt to be small (ref. 6). The resonance effect discussed in reference 7 only becomes important for the frequencies considered here at Mach numbers near unity, and thus requires no consideration. The data have not been corrected for blockage, turbulence, or support interference although the latter may have a sizeable magnitude at the higher angles of attack.

REDUCTION OF DATA

From a continuous record taken of the displacement of the model and the rolling moment and yawing moment after initial displacement (see fig. 6), the phase angle relationship of these moments to the model displacement were determined. Reduction of the data by means of the phase angle approach was simplified in that the inertia effects were eliminated before testing. In addition, the oscillation frequency and the ratio of moment amplitude to displacement amplitude were also determined. Evaluation of the phase angle was made by measuring the phase relationship of corresponding peaks of the moment and motion traces over approximately 30 cycles and averaging the result. The acceleration derivatives $C_{n_{\dot{\beta}}}$ and $C_{l_{\dot{\beta}}}$ corresponded to the moment components in phase with the model displacement whereas the oscillatory derivatives $C_{n_{\beta}}$ and $C_{l_{\beta}}$ corresponded to the out-of-phase components. Equations which illustrate this phase relationship and which were used for reducing the rolling moment data, for example, are as follows:

$$C_{l_{\beta}} = \frac{L'_o}{y_o} \frac{V \sin \phi}{57.3(2\pi f)qSb}$$

$$C_{l_{\dot{\beta}}} = -\frac{L'_o}{y_o} \frac{\cos \phi}{\rho S \pi^2 f^2 b^2}$$

The term L'_o/y_o represents the ratio of the rolling-moment amplitude to the amplitude of model displacement at any specified time. Similar equations were used for reducing the yawing-moment data.

The two expressions for $C_{l_{\beta}}$ and $C_{l_{\dot{\beta}}}$ were obtained assuming that the trace of model displacement and hence the traces of rolling and yawing moment were of constant amplitude. Neglecting the effect of damping on the oscillation was felt to be a reasonable assumption, since

the trace of model displacement indicated only a small reduction in amplitude for successive cycles. (For example, see fig. 6.)

RESULTS AND DISCUSSION

Basic Data

Experimental lift, drag, and pitching-moment results for each of the three wings at zero sideslip are presented in figure 7. The data are about as would be expected; however, the large drag levels indicated for all three wings in the low angle-of-attack range are believed to be the result of the influence of the canopies covering the strain-gage balance. In addition, a rather large value of lift coefficient is indicated for the 45° swept wing at zero angle of attack. In reference 8, support tares are available for a similar wing having an identical plan form and area but a different airfoil section. The tare values shown would appear to account for a large portion of the lift coefficient at $\alpha = 0^\circ$ indicated in the present data.

Acceleration Derivatives

Effect of plan form.- The sideslip acceleration derivatives $C_{n_{\dot{\beta}}}$ and $C_{l_{\dot{\beta}}}$ for each of the three wings are presented in figure 8 as functions of angle of attack. These results are for a frequency of 2.3 cycles per second. The unswept wing results appear to be of small magnitude and fairly constant through the angle-of-attack range. Although data for $C_{n_{\dot{\beta}}}$ for the unswept wing are presented up to an angle of attack of 16°, the rolling-moment data are not, because these data were too erratic for reduction above $\alpha = 10^\circ$. Above $\alpha = 10^\circ$ large fluctuations were obtained in the rolling-moment trace for the wind-on condition prior to permitting the test apparatus to oscillate. These fluctuations were believed to be caused by separation as evidenced by the break in the lift curve at $\alpha = 10^\circ$. (See fig. 7.)

For the swept and triangular wings the values of the acceleration derivatives were small and almost constant in the low angle-of-attack range as were the values for the unswept wing. In the high angle-of-attack range, however, the derivatives for both wings experience a rapid increase in value with increase in angle of attack and acquire values of appreciable magnitude. The values for the 60° triangular wing develop at a higher angle of attack and increase more gradually than those for the 45° swept wing, but reach higher values at the maximum test angles of attack. These derivatives appear to develop in proportion to the

degree that the trailing vortices are separated from the surface of the wing. For the triangular wing, this effect takes place at a very low angle of attack and increases gradually to maximum lift. In the case of the 45° swept wing, the beginning of the separation of the vortices from the surface of the wing is delayed to a higher angle of attack, but the separation increases more rapidly with angle of attack, and involves a less steady flow, once begun. The 45° swept wing has a lower angle of attack for maximum lift than the 60° triangular wing, of course. Reference 9 shows tuft-grid pictures of the flow behind a 60° triangular wing oscillating in sideslip such that the sideslip angle is always the negative of the azimuth angle. These pictures show a decided roughness, and inward displacement relative to the tip, of the vortex trailing from the leading half-span of the wing. This roughness persists until the model has returned and passed considerably beyond zero sideslip indicating the presence of a lag effect that may be considerably different from purely potential flow.

Some indication of the significance of these acceleration derivatives can be obtained by considering their magnitude relative to commonly encountered values of the yawing derivatives with which they combine approximately in the Dutch roll mode of the lateral motion. These approximate combinations of derivatives are $C_{n_r} - C_{n_{\dot{\beta}}}$ and $C_{l_r} - C_{l_{\dot{\beta}}}$ in which form they are frequently measured in the more usual type of oscillation test. A common value for the derivative C_{n_r} for a model with a vertical tail is from -0.2 to -0.4, and the derivative C_{l_r} for a 60° triangular wing may range from 0.05 to -0.17 (ref. 10). The values of $C_{n_{\dot{\beta}}}$ and $C_{l_{\dot{\beta}}}$ measured for the 60° triangular wing reach values of 0.75 and -1.16, respectively, at the higher angles of attack. These values are several times as large as the yawing derivatives quoted, and thus should be of considerable importance in lateral-stability calculations. A similar measure of the importance of the sideslip acceleration derivatives is given in reference 2.

In addition to the rolling- and yawing-moment measurements, two tests were conducted which provided some additional information on the acceleration effects. These tests consisted of measurements of the pitching moment at $\alpha = 0°$ and $\alpha = 24°$ for the 60° triangular wing. Only small amplitudes of oscillation were evident in the pitching-moment traces at these two angles of attack, and this fact indicates that acceleration in sideslip had but little influence on the wing chordwise center of pressure.

Effect of frequency.- An indication of the effect of frequency of oscillation on the derivatives $C_{n_{\dot{\beta}}}$ and $C_{l_{\dot{\beta}}}$ for the 60° triangular wing can be obtained from figure 9, which presents the oscillatory derivatives plotted against angle of attack for average frequencies of 1.4

and 2.3 cycles per second. Some difference existed in the values of the oscillation frequency between the different test points as a result of variations in the aerodynamic forces; however, for all the data obtained, variations in frequency occurred within the ranges of 1.3 to 1.5 cycles per second and 2.15 to 2.45 cycles per second.

The data for the acceleration derivatives $C_{n_{\dot{\beta}}}$ and $C_{l_{\dot{\beta}}}$ are generally in agreement for the two frequencies of oscillation up to an angle of attack of about 26°. Above $\alpha = 26°$, however, this is no longer true. A comparison of the values of the sideslip acceleration derivatives for the two frequencies at angles of attack above 26° indicates that the magnitudes of the derivatives associated with the lower frequency reached values approximately twice as large as those associated with the higher frequency. Although the difference in the results for these two tests are believed to be caused principally by the difference in frequency of oscillation, it should be pointed out that the amplitude of the sideslip angle β was different for the two frequencies in direct proportion to the frequency. The test results for a frequency of 1.4 cycles per second were obtained merely by changing the spring constant of the oscillation apparatus while retaining the same forward velocity and amplitude of model displacement.

Sideslip Derivatives

Comparisons of the oscillatory results for C_{n_β} and C_{l_β} for each of the three wings tested with data obtained from static sideslip tests, which correspond to a zero frequency of oscillation, are presented in figures 10, 11, and 12. The oscillatory results for the straight and 45° swept wings were obtained for a frequency of 2.3 cycles per second, and for the 60° triangular wing for both 1.4 and 2.3 cycles per second. The oscillation and static sideslip results for C_{n_β} and C_{l_β} for the unswept wing (fig. 10) are in agreement throughout the angle-of-attack range indicating a negligible influence of unsteady motion. No appreciable separation effects existed on this wing throughout the angle-of-attack range to the stall, of course, and the values of the acceleration derivatives were also small. Agreement is also shown for the static and oscillatory C_{n_β} for the 45° swept wing (fig. 11) with the exception of a small difference occurring at the higher angles of attack. The C_{l_β} results, however, show appreciable unsteady effects throughout the angle-of-attack range. At an angle of attack of 20°, the value of C_{l_β} for the oscillatory result is 0 as compared with 0.0025 for the static case.

The results for $C_{n_{\dot{\beta}}}$ and $C_{l_{\dot{\beta}}}$ for the 60° triangular wing (fig. 12) show a much clearer effect of unsteady motion than the results for either the unswept or 45° swept wings. This unsteady effect becomes progressively greater at the higher angles of attack in much the same way as the increase of the $\dot{\beta}$ derivatives with angle of attack (fig. 8). The static or zero frequency result indicates a change in the sign of $C_{n_{\dot{\beta}}}$ and $C_{l_{\dot{\beta}}}$ at angles of attack of 27° and 26°, respectively, whereas the oscillatory results indicate no change in sign. The oscillatory derivatives for 1.4 cycles per second are nearer the static derivatives than the oscillatory derivatives for 2.3 cycles per second which is as might be expected. Additional tests, particularly at higher Reynolds numbers, are needed, in order to establish the nature of the unsteady effects on the $C_{n_{\dot{\beta}}}$ and $C_{l_{\dot{\beta}}}$ of these wings.

The high angle-of-attack oscillatory results at a frequency of 2.3 cycles per second for both $C_{n_{\dot{\beta}}}$ and $C_{l_{\dot{\beta}}}$ for this wing are probably the most accurate of any of the high angle-of-attack data for the three wings, in that the records of the rolling and yawing moment were but slightly distorted by separated flow conditions.

CONCLUSIONS

The results of a low-speed wind-tunnel investigation to determine representative variations of the sideslip acceleration derivatives with angle of attack for a 60° triangular, a 45° swept, and an unswept wing indicate the following conclusions:

1. The magnitude of the sideslip acceleration derivatives encountered and the effect of wing plan form on these derivatives was small in the low angle-of-attack range. In the high angle-of-attack range, the swept and triangular plan forms had values of the sideslip acceleration derivatives that were large in comparison with the other stability derivatives with which they are generally combined in the lateral-stability calculations. These acceleration derivatives increased with angle of attack at a much greater rate for the high angle-of-attack range than for the low angle-of-attack range. The acceleration derivatives for the unswept plan form were small throughout the angle-of-attack range in comparison with the values for the wings with swept and triangular plan forms.

2. For the 60° triangular wing, a reduction in the frequency of oscillation of 40 percent influenced the acceleration derivatives mainly at the angles of attack higher than 26°. At these high angles, the magnitudes of the sideslip acceleration derivatives associated with the

lower frequency reached values approximately twice as large as those associated with the higher frequency.

3. A comparison of the oscillatory results for the lateral-stability derivatives C_{n_β} and C_{l_β} with static sideslip results for the 60° triangular wing indicated agreement at the low angles of attack where the acceleration derivatives were small and a definite departure at the high angles of attack. Similar trends were evident for the 45° swept wing. Agreement between the oscillatory and static sideslip derivatives was obtained for the unswept wing throughout the angle-of-attack range, indicating that the unsteady effects were small for this wing.

Langley Aeronautical Laboratory,
National Advisory Committee for Aeronautics,
Langley Field, Va., December 31, 1954.

REFERENCES

1. Bird, John D., Jaquet, Byron M., and Cowan, John W.: Effect of Fuselage and Tail Surfaces on Low-Speed Yawing Characteristics of a Swept-Wing Model As Determined in Curved-Flow Test Section of the Langley Stability Tunnel. NACA TN 2483, 1951. (Supersedes NACA RM L8G13.)

2. Johnson, Joseph L., Jr.: Low-Speed Measurements of Rolling and Yawing Stability Derivatives of a 60° Delta-Wing Model. NACA RM L54G27, 1954.

3. Fisher, Lewis R., and Fletcher, Herman S.: Effect of Lag of Sidewash on the Vertical-Tail Contribution to Oscillatory Damping in Yaw of Airplane Models. NACA TN 3356, 1955.

4. Campbell, John P., and Woodling, Carroll H.: Calculated Effects of the Lateral Acceleration Derivatives on the Dynamic Lateral Stability of a Delta-Wing Airplane. NACA RM L54K26, 1955.

5. Silverstein, Abe, and White, James A.: Wind-Tunnel Interference With Particular Reference to Off-Center Positions of the Wing and to the Downwash at the Tail. NACA Rep. 547, 1936.

6. Evans, J. M.: Stability Derivatives. Wind Tunnel Interference on the Lateral Derivatives l_p, l_r and l_v with Particular Reference to l_p. Rep. ACA-33, Australian Council for Aeronautics, Mar. 1947.

7. Runyan, Harry L., Woolston, Donald S., and Rainey, A. Gerald: A Theoretical and Experimental Study of Wind-Tunnel-Wall Effects on Oscillating Air Forces for Two-Dimensional Subsonic Compressible Flow. NACA RM L52I17a, 1953.

8. Jaquet, Byron M.: Effect of Linear Spanwise Variations of Twist and Circular-Arc Camber on Low-Speed Static Stability, Rolling, and Yawing Characteristics of a 45° Sweptback Wing of Aspect Ratio 4 and Taper Ratio 0.6. NACA TN 2775, 1952.

9. Bird, John D., and Riley, Donald R.: Some Experiments on Visualization of Flow Fields Behind Low-Aspect-Ratio Wings by Means of a Tuft Grid. NACA TN 2674, 1952.

10. Goodman, Alex: Effect of Various Outboard and Central Fins on Low-Speed Yawing Stability Derivatives of a 60° Delta-Wing Model. NACA RM L50E12a, 1950.

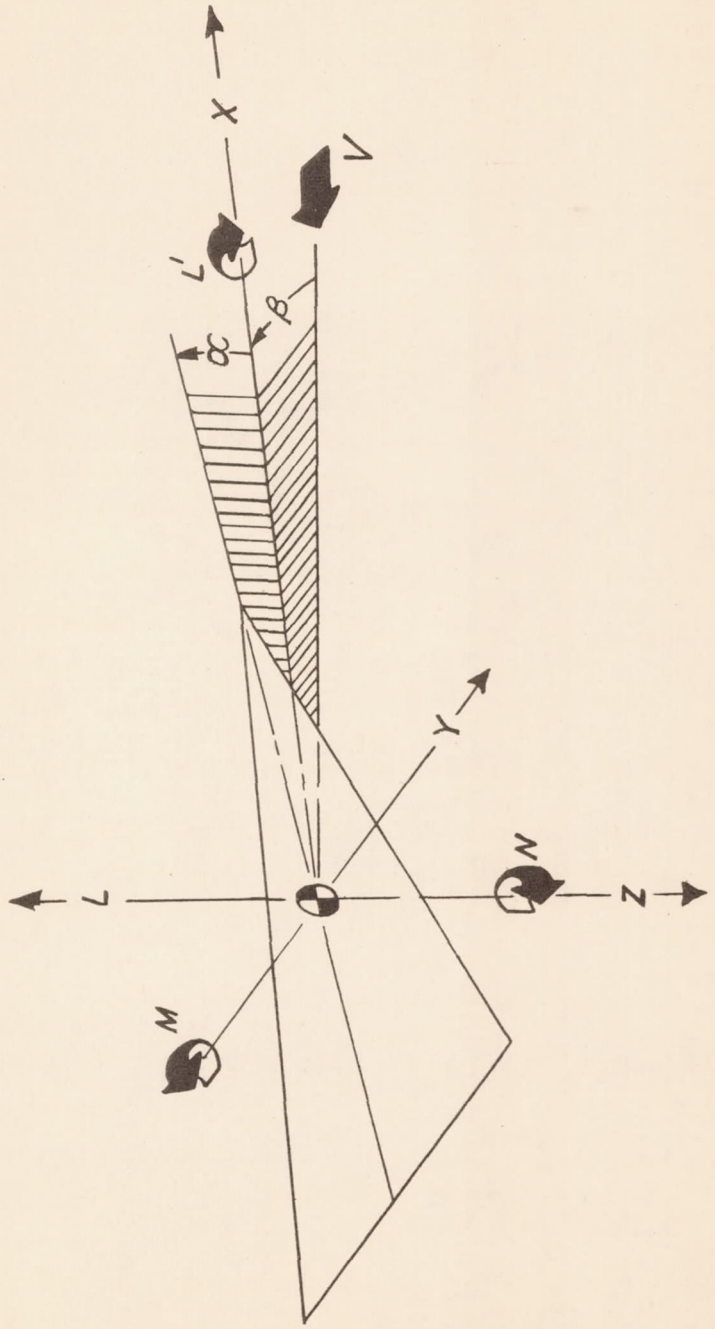

Figure 1.- Sketch of axes used. Arrows indicate positive direction of forces, moment, and angles.

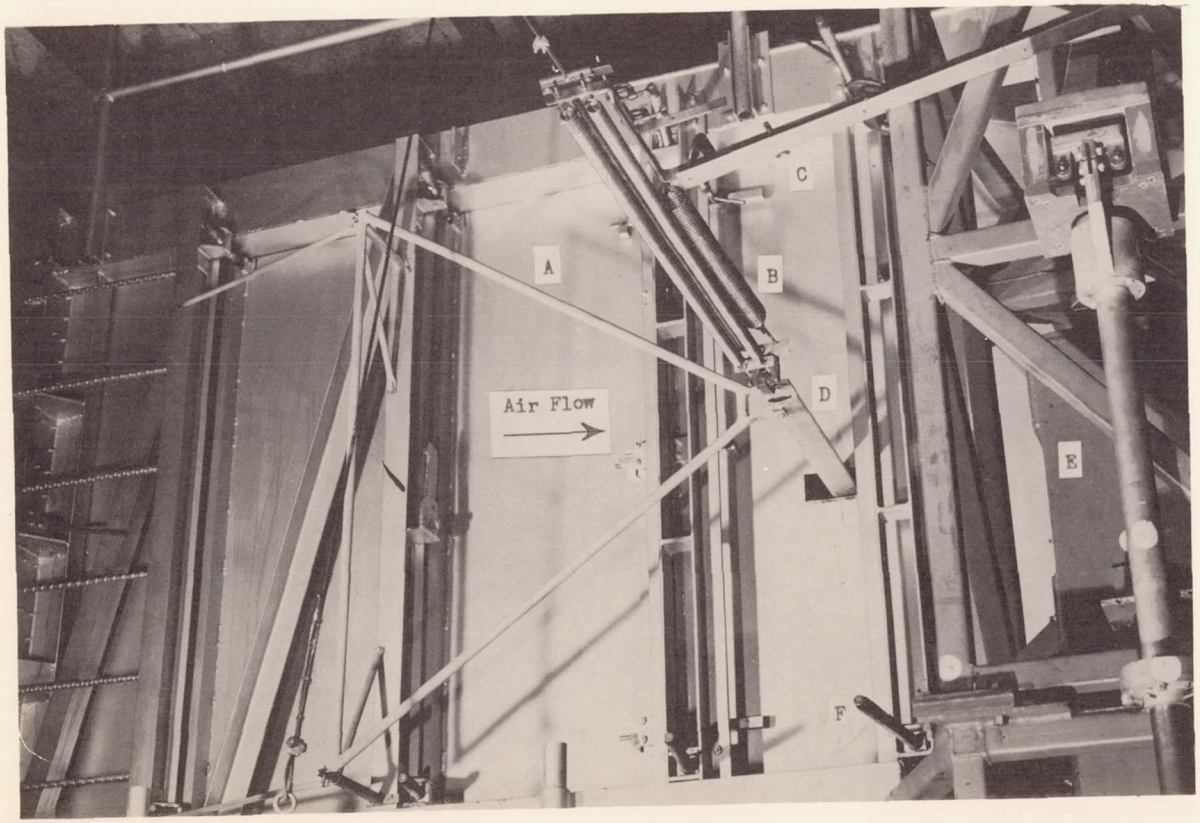

A Swinging arm
B Coiled springs
C Temporary bracing for springs
D Streamlined strut
E Portion of conventional six-component balance
F Jack screw for deflecting flexible walls

(a) Left side view looking upstream. L-85318.1

Figure 2.- Side views of the 6- by 6-foot test section of Langley stability tunnel showing details of the oscillation test setup and equipment employed. (This test section is equipped with flexible steel walls that may be curved by means of jack screws to permit an evaluation of the steady-state pitching and yawing stability derivatives.)

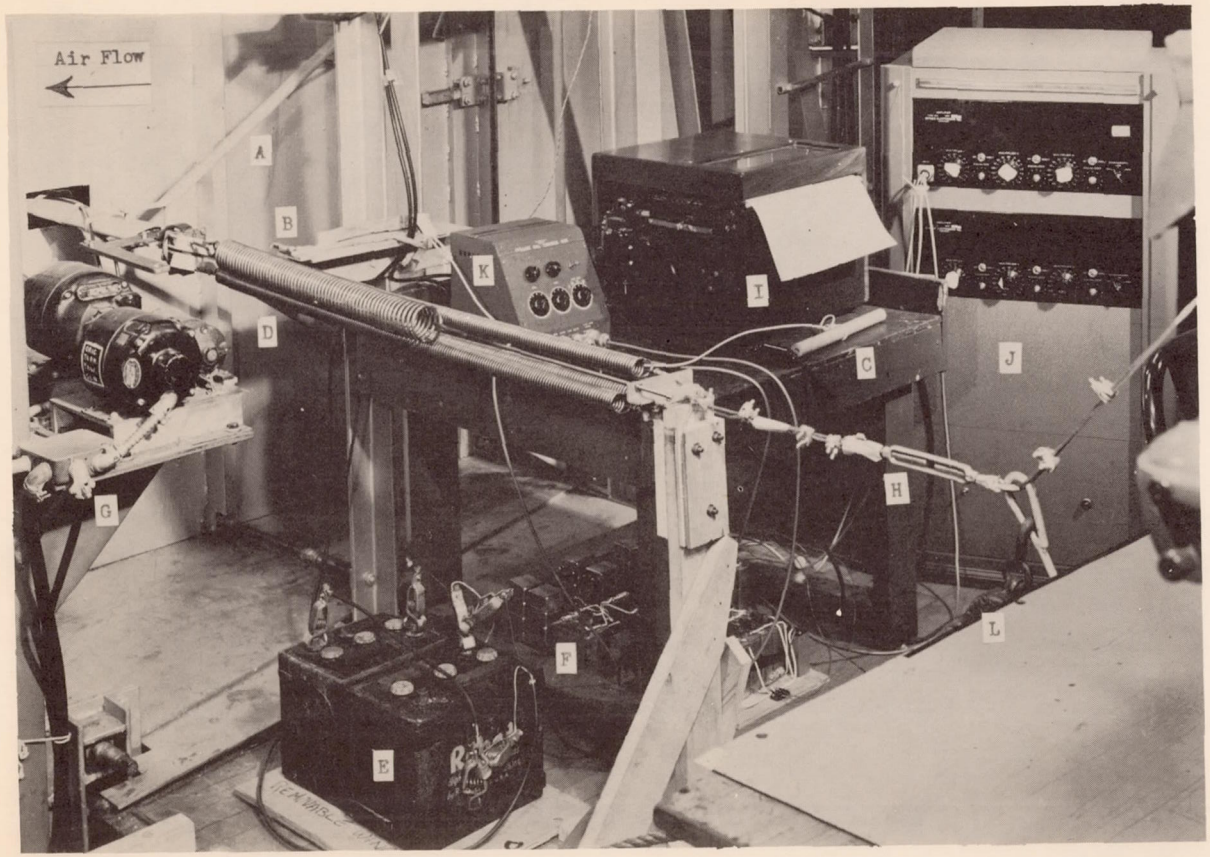

A Swinging arm
B Trigger mechanism
C Trigger release handle
D Coiled springs
E 6-volt storage batteries
F Filters
G Portion of conventional six-component balance system
H Cable support for springs
I Multi-channel ink recorder
J Amplifier
K Control box
L Rope fall for providing initial deflection of test rig

(b) Right side view looking upstream. L-85319.1

Figure 2.- Concluded.

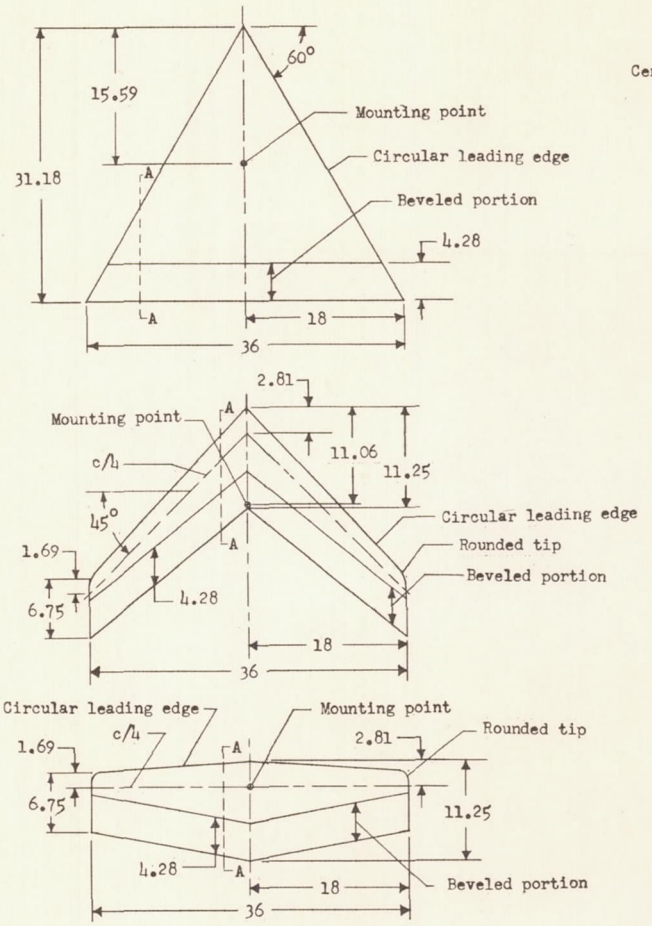

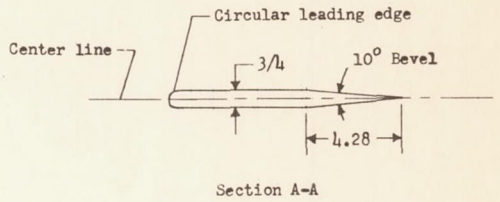

Section A-A

Triangular Wing	
Aspect ratio	2.31
Leading edge sweep angle, deg.	60
Dihedral angle, deg.	0
Twist, deg.	0
Airfoil section	Flat plate
Area, sq. in.	561.20
Span, in.	36.00
Mean aerodynamic chord, in.	20.79

Swept Wing	
Aspect ratio	4.0
Taper ratio	0.6
Quarter chord sweep angle, deg.	45
Dihedral angle, deg.	0
Twist, deg.	0
Airfoil section	Flat plate
Area, sq. in.	324
Span, in.	36
Mean aerodynamic chord	9.19

Unswept Wing	
Aspect ratio	4.0
Taper ratio	0.6
Quarter chord sweep angle, deg.	0
Dihedral angle, deg.	0
Twist, deg.	0
Airfoil section	Flat plate
Area, sq. in.	324
Span, in.	36
Mean aerodynamic chord	9.19

Figure 3.- Sketches and geometric characteristics of the three wing models investigated (all dimensions are in inches).

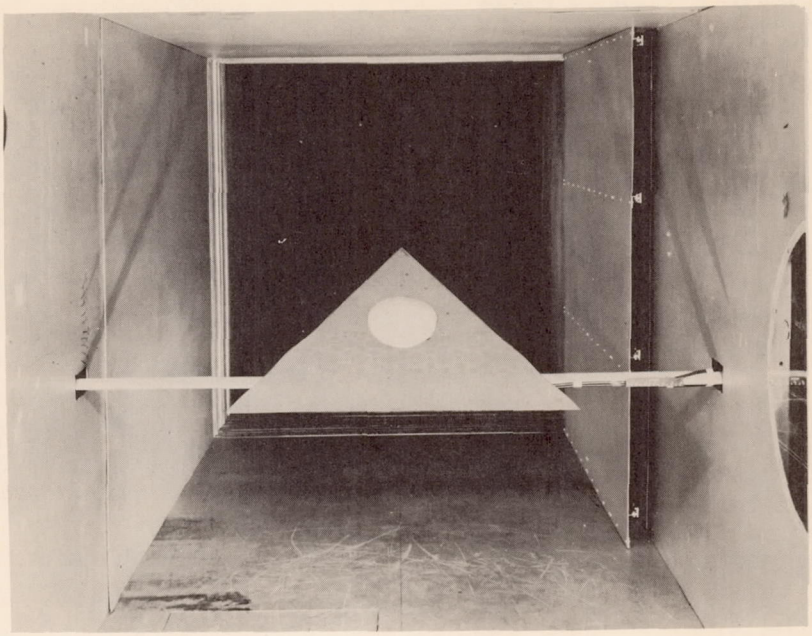

(a) 60° triangular wing. L-85320

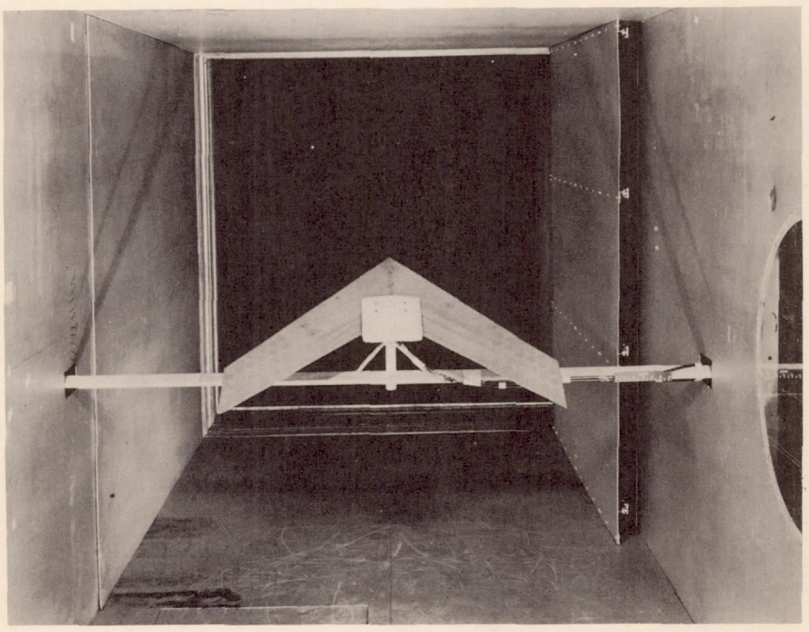

(b) 45° swept wing. L-85321

Figure 4.- Photographs of the three wing models mounted on the oscillation test rig in the 6- by 6-foot test section of the Langley stability tunnel.

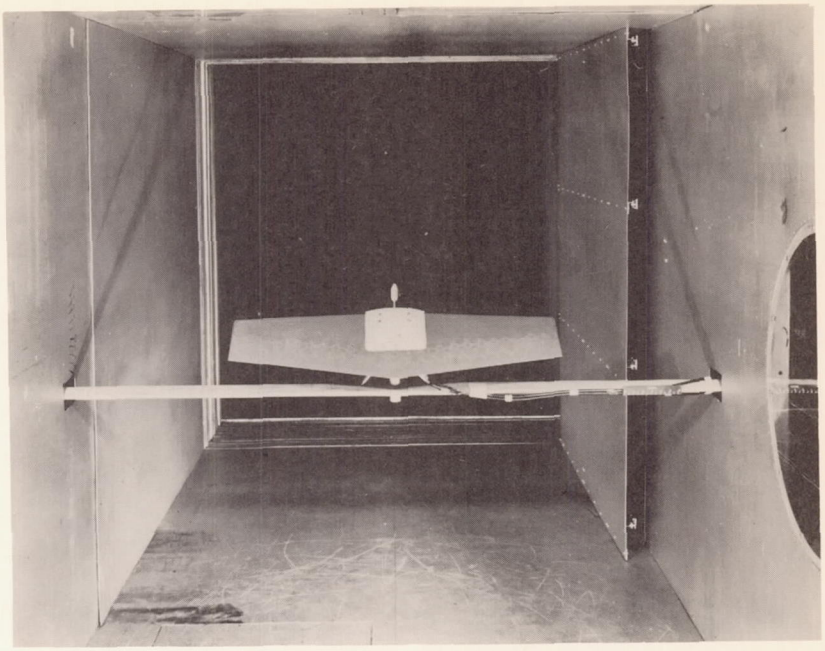

(c) Unswept wing. L-85322

Figure 4.- Concluded.

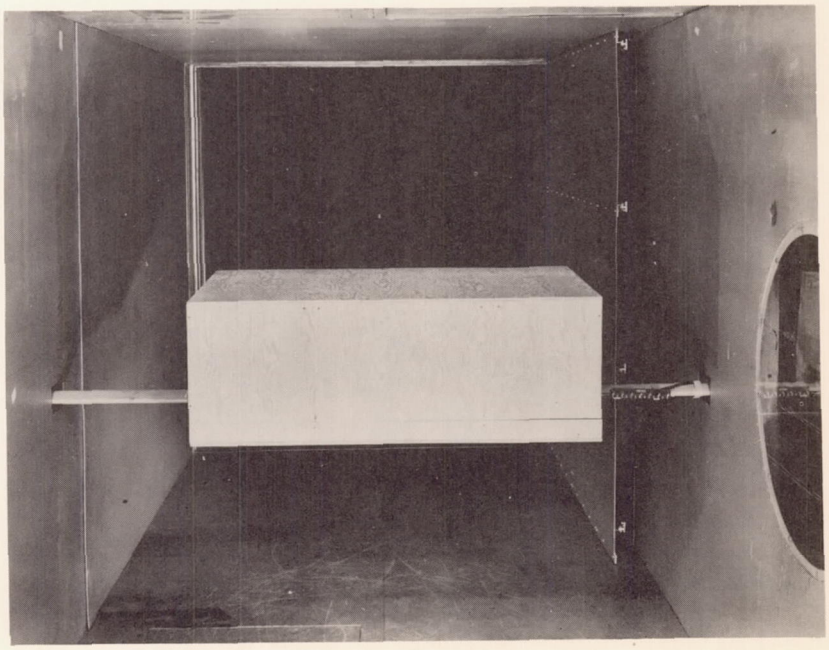

L-85323

Figure 5.- Photograph of the plywood box which completely encased each of the three wing models for tests at zero tunnel airspeed.

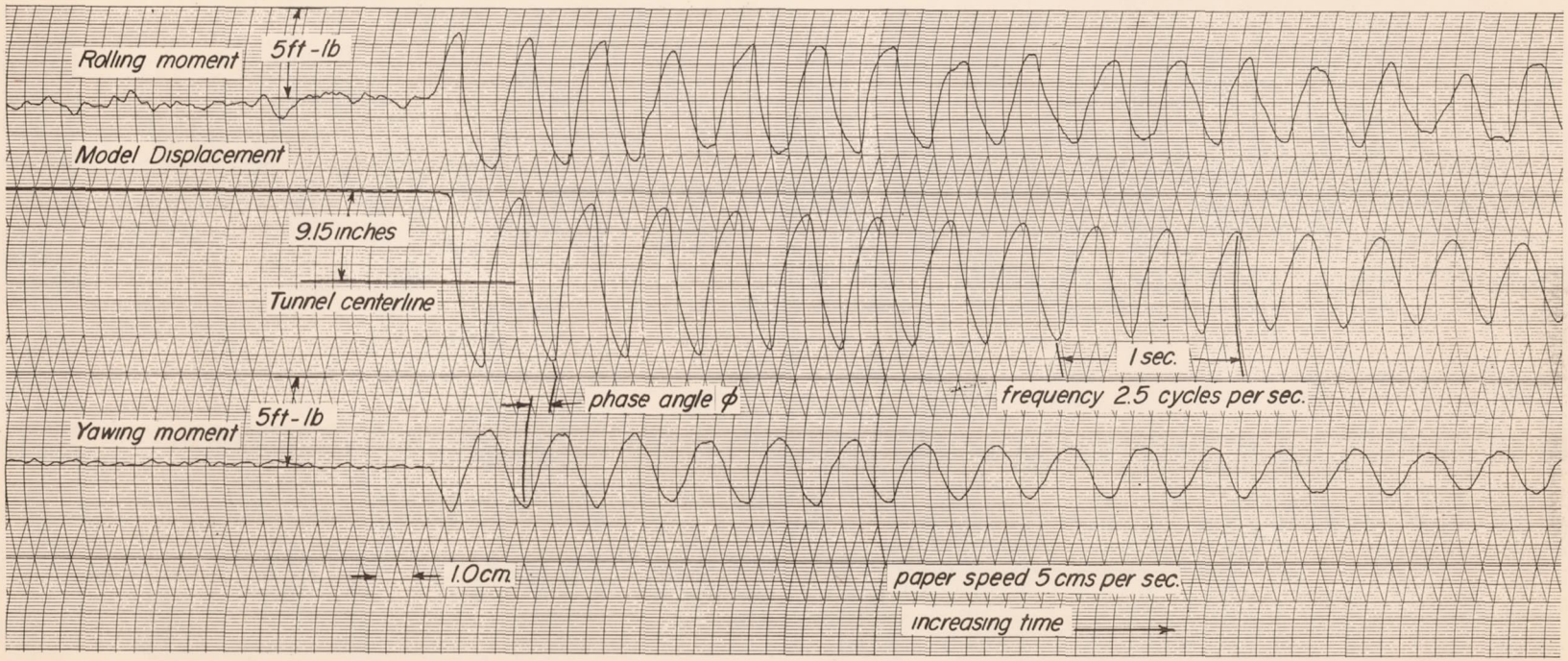

Figure 6.- Sample record obtained for 60° triangular wing at an angle of attack of 24°. q = 39.7 pounds per square foot.

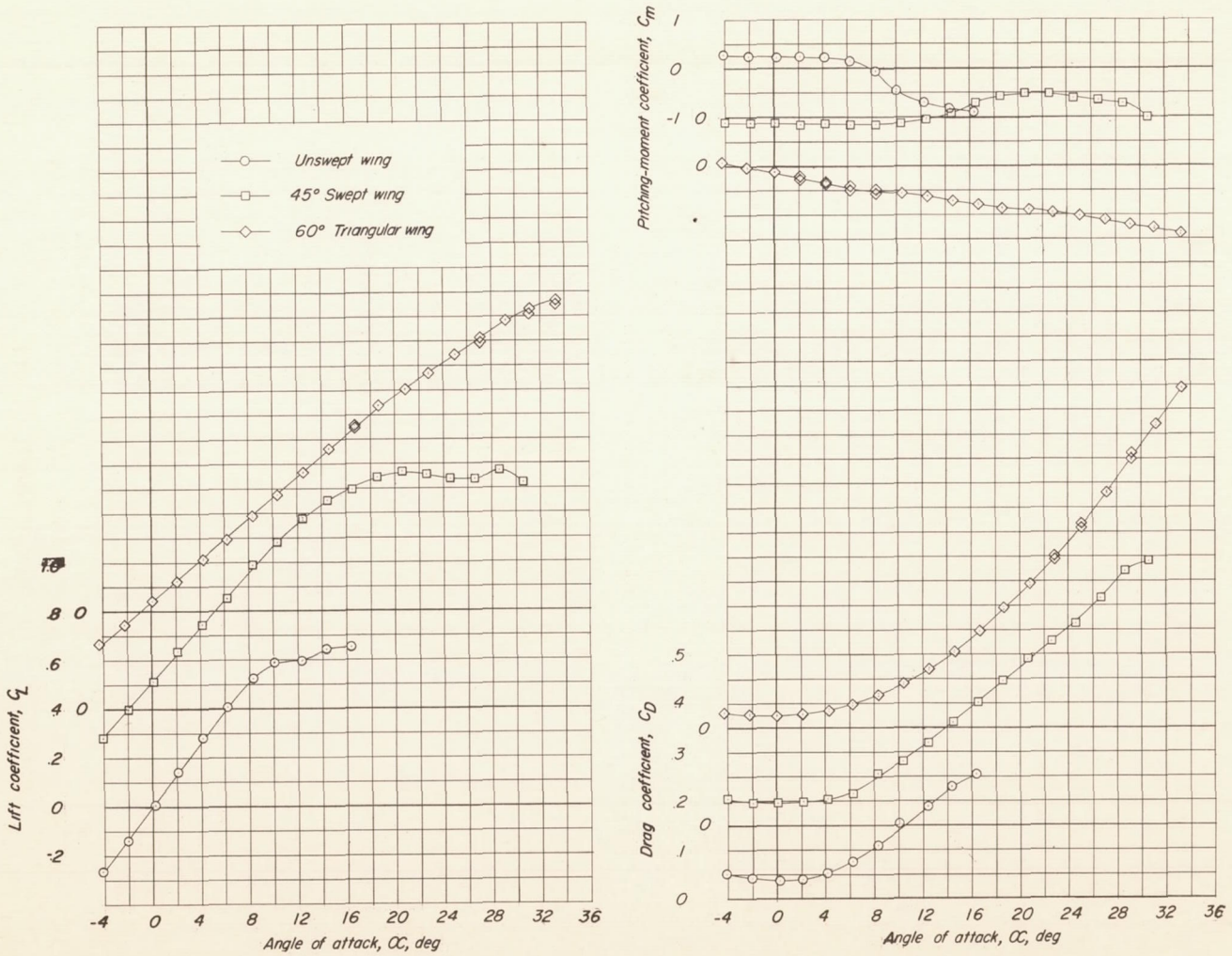

Figure 7.- Lift, drag, and pitching-moment characteristics as a function of angle of attack for the unswept, the 45° sweptback, and the 60° triangular wings. $\beta = 0°$.

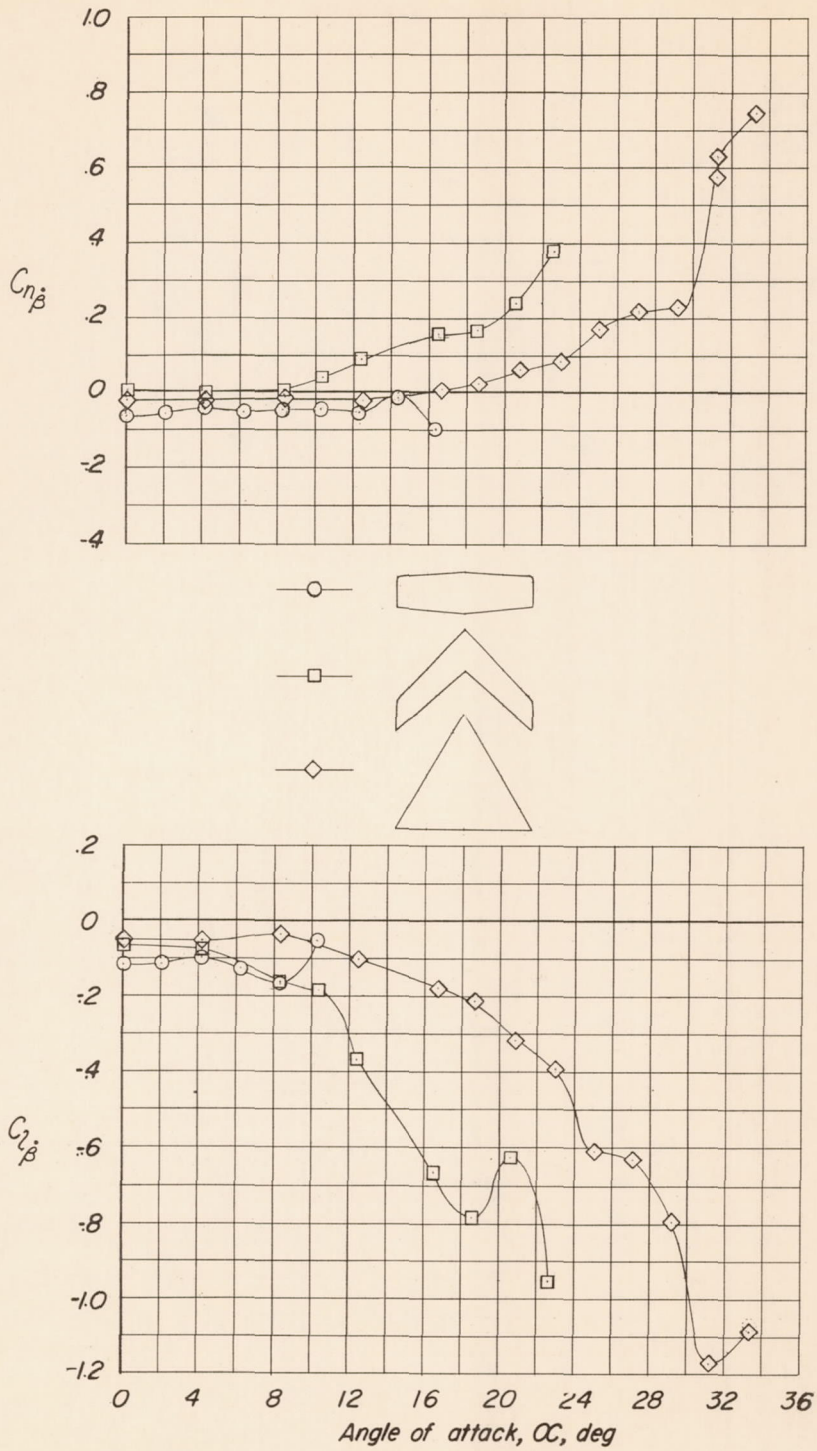

Figure 8.- Sideslip acceleration derivatives $C_{n_{\dot{\beta}}}$ and $C_{l_{\dot{\beta}}}$ for the three wings investigated as functions of angle of attack. Average frequency of oscillation was about 2.3 cycles per second.

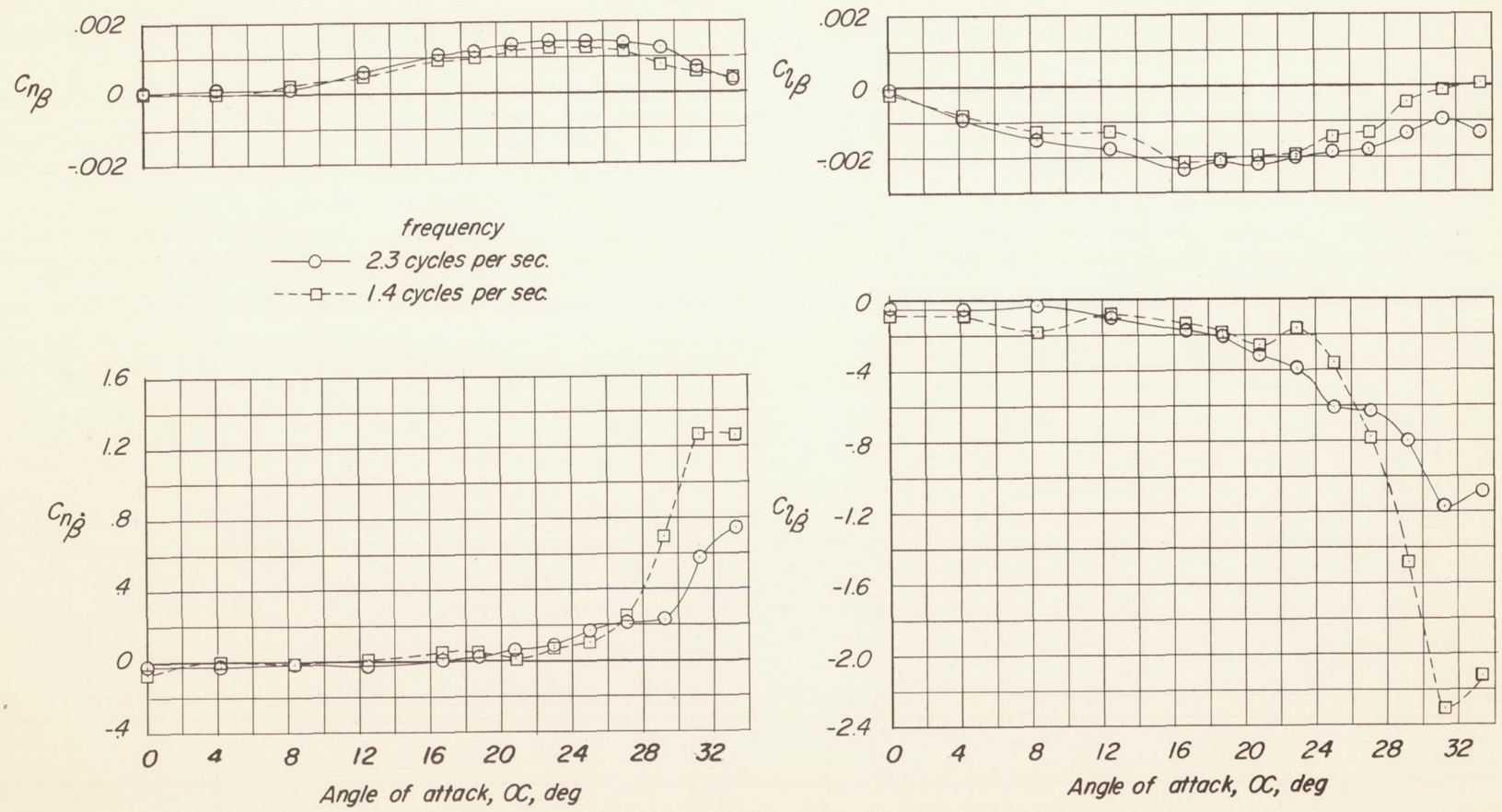

Figure 9.- Comparison of the oscillatory derivatives of the 60° triangular wing for two frequencies of oscillation, 1.4 and 2.3 cycles per second.

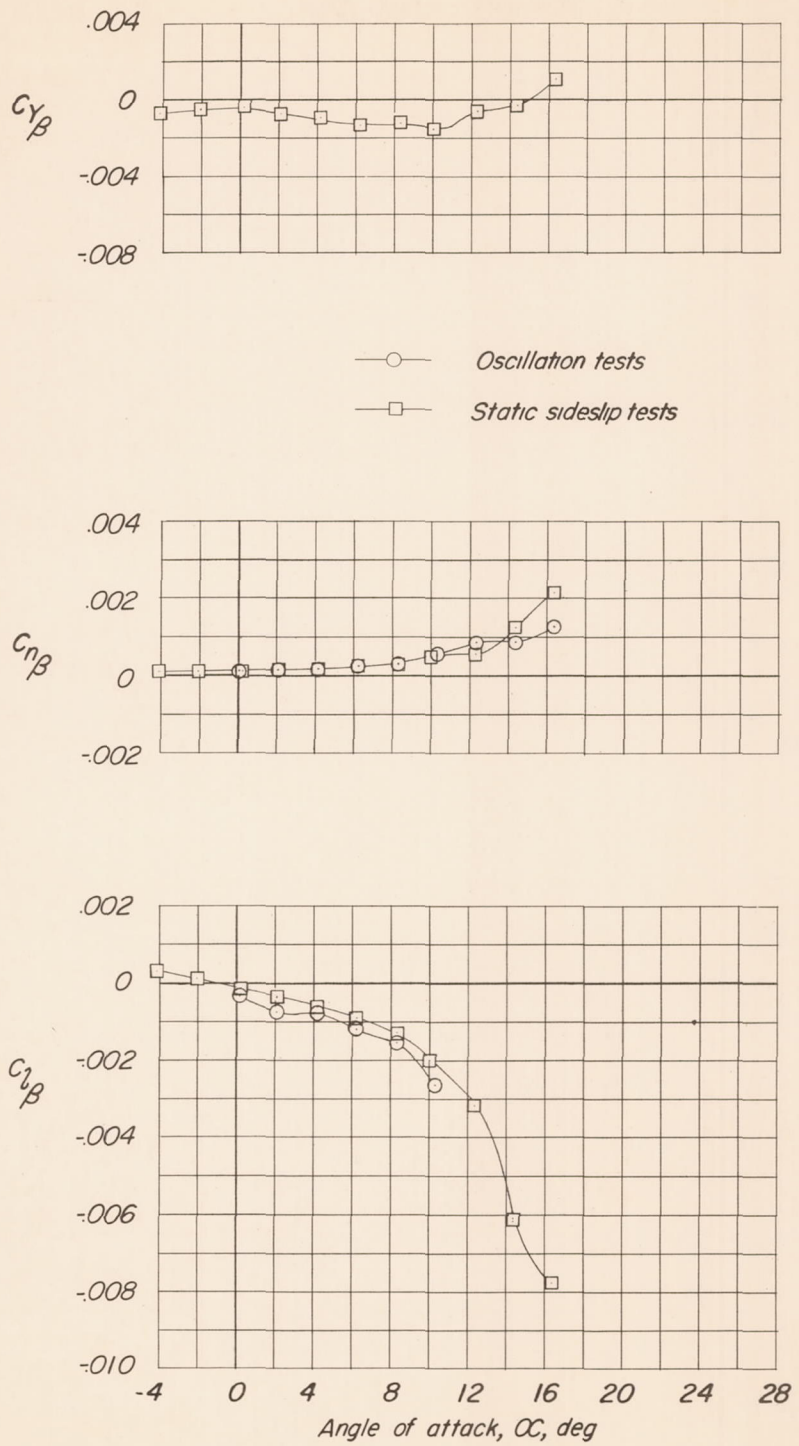

Figure 10.- Comparison of the oscillatory test results for C_{n_β} and C_{l_β} with static sideslip test data for the unswept wing investigated. Average frequency of oscillation was about 2.3 cycles per second.

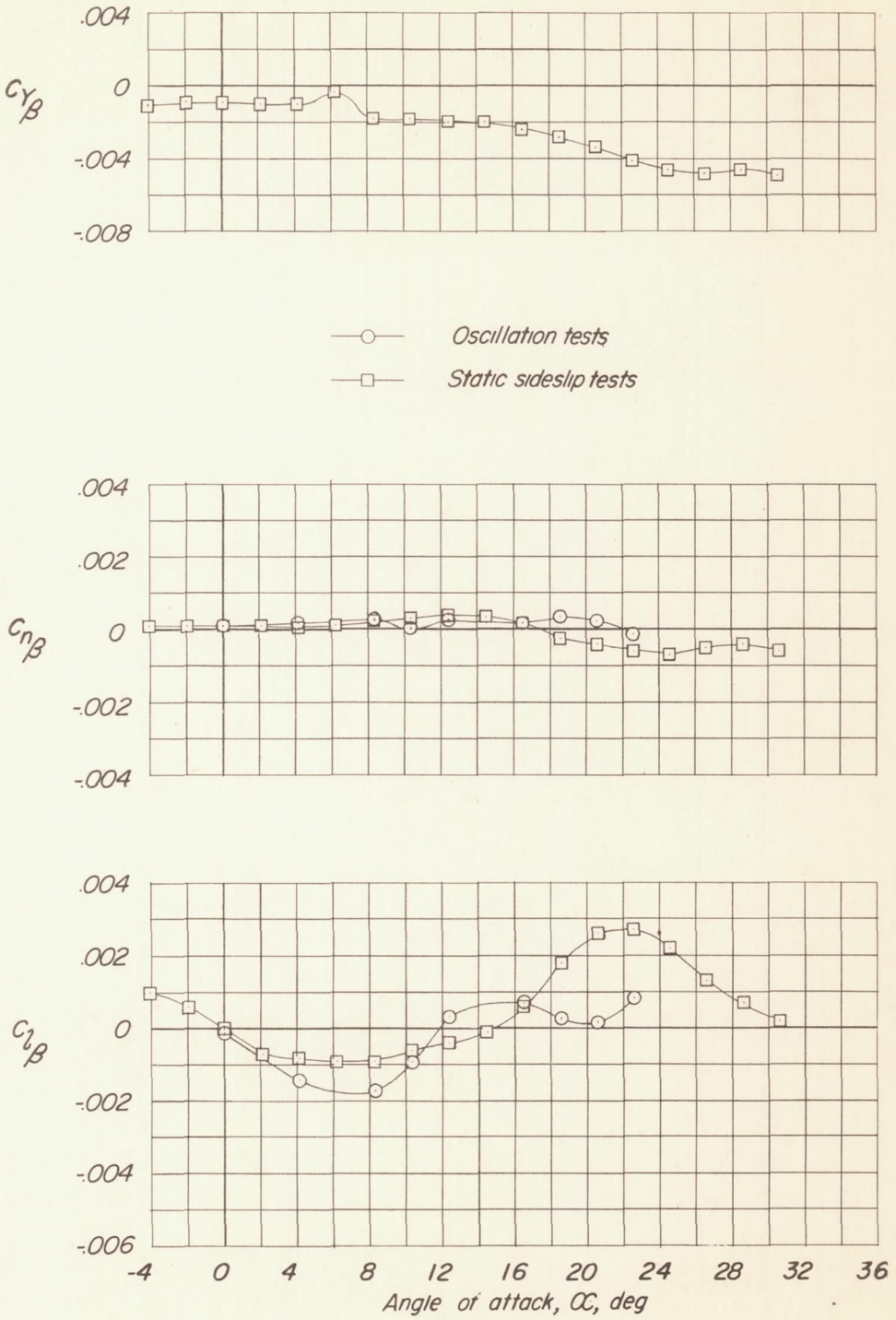

Figure 11.- Comparison of the oscillatory test results for C_{n_β} and C_{l_β} with static sideslip test data for the 45° swept wing. Average frequency of oscillation was about 2.3 cycles per second.

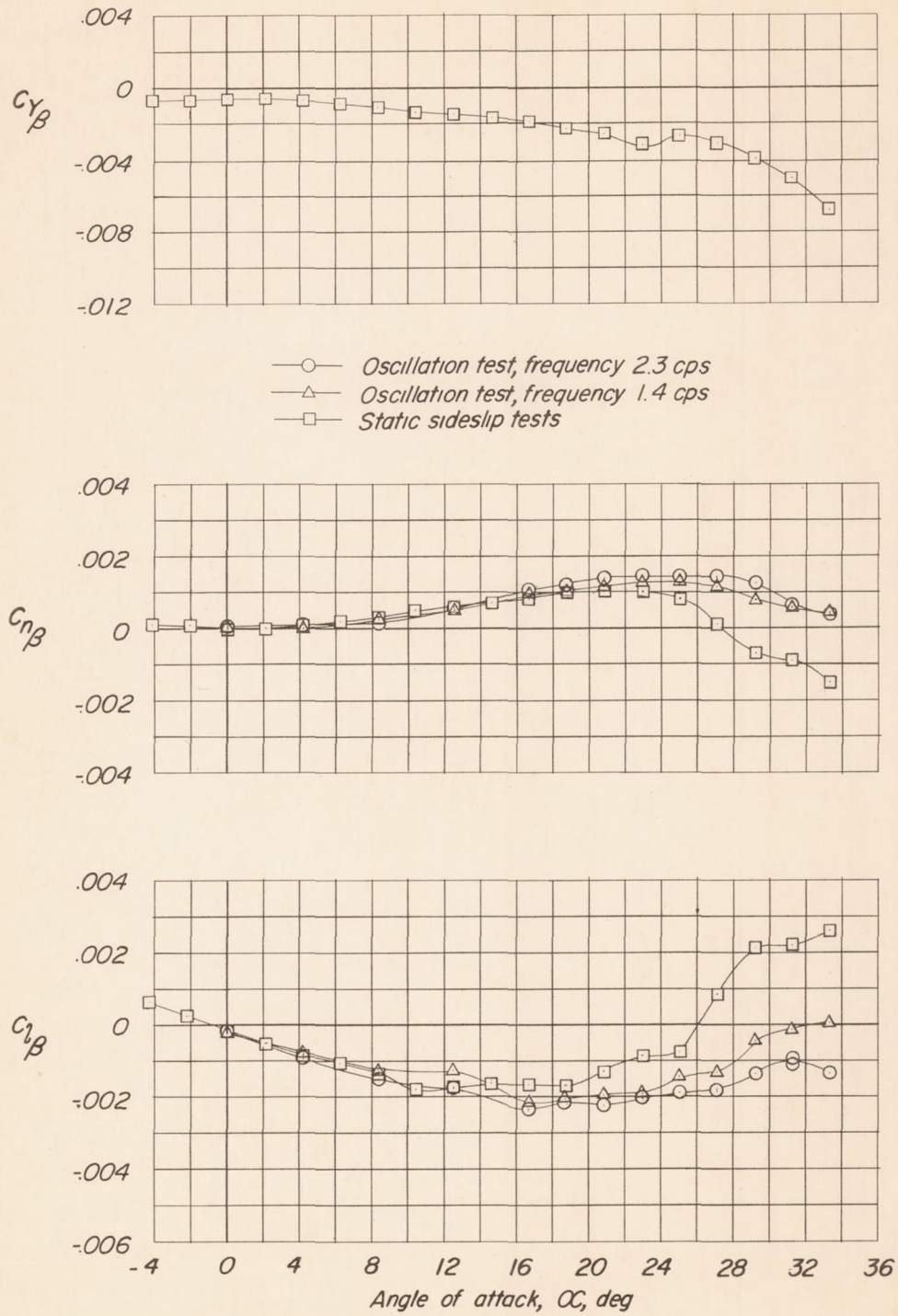

Figure 12.- Comparison of the oscillatory test results for C_{n_β} and C_{l_β} at two frequencies with static sideslip test data for the 60° triangular wing investigated.

NACA-Langley - 3-30-55 - 350